CHAPTER II

EXCITED-STATE INTERMOLECULAR PROTON TRANSFER REACTIONS IN 7-AZAINDOLE WITH METHANOL CLUSTERS

2.1 Introduction

Most of previous reports [13,15-17,29] have paid much attention to 7AI molecule because of its simple structure in being employed as a model compound to reveal a key reaction for chemical mutagenesis of DNA base pairs [50]. In addition, 7AI molecule is an important bicyclic azaaromatic molecule consisting of pyrrole (proton donor) and pyridine (proton acceptor) rings. The 7AI with solvent clusters, which have been extensively studied in solvents such as ammonia [51], water [13,29,32,52-56], and alcohol (especially ethanol [33] and methanol [31,34-36,57-58]), are prototypes for understanding the ESInterPT/HT reactions as illustrated in Figure 2.1.

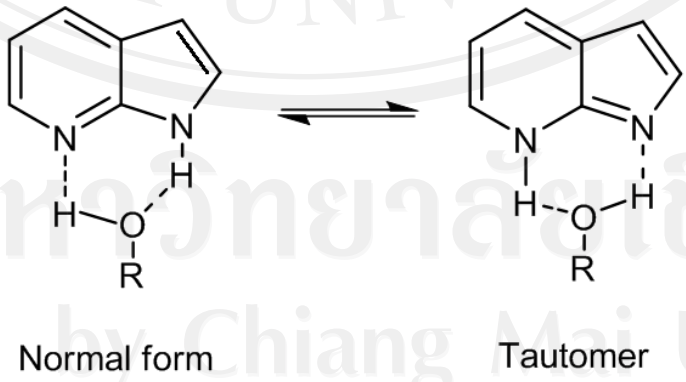

Figure 2.1 Scheme of intermolecular PT/HT reaction of 7-azaindole with alcohol

However, bulk property approach is still difficult to provide quantitative information about the multiple-PT/HT process. Thus, model compounds consisting of 7AI and solvents can be employed to clarify complicated systems using theoretical calculations.

Recently, Sakota *et al.* [31-32,35-36,58] have studied 7AI and its clusters both experimental and theoretical to obtain information on the PT/HT reaction using supersonic jet-cool apparatus and structure calculations. Their results showed that the ESPT/HT reactions occurred by solvent-induced molecules involving cooperative hydrogen-bonded network in $7AI(MeOH)_{n=1-3}$ clusters evidenced by IR-UV ion-dip spectroscopy. In addition, they found that the observation of the visible fluorescence due to the multiple-PT/HT is cluster-size selective; the $7AI(MeOH)_2$ complex undergoes excited-state triple PT/HT (ESTPT/HT) reaction efficiently along hydrogen-bonded network [36]. However, their data of the ESPT/HT reaction could not provide sufficient dynamic information, particularly reaction pathways and time evolution [59-63] in the ultrafast time scale. Dynamics simulations can be employed to explore this challenging system in order to understand the ESPT/HT mechanism, as have been done, for example, by Kina *et al*. [29] who used *ab initio* molecular dynamics simulation (AIMD) for studying the ESPT reaction of 7AI in water solution. Theoretical investigations can provide more elaborated pictures in molecular level than experimental results by themselves. Therefore, the combination of both methods [29,32] can serve as a powerful tool to clarify detailed mechanisms of the PT/HT processes. These reactions in the excited state can exhibit either the ESPT or ESHT depending on energy differences of ground (S_0) and excited states ($S_{\pi\pi^*}$ and $S_{\pi\sigma^*}$) in the target systems. These states play important role in determining the nature

of the excited-state reactions when the ESPT occurs through the $S_{\pi\pi^*}$ state, whereas the ESHT occurs through $S_{\pi\sigma^*}$ state [26,64-66]. Particularly, it has been pointed out in previous investigations [32,67] that the energy paths of $S_{\pi\sigma^*}$ state lies well above the $S_{\pi\pi^*}$ state with no crossing between them.

In this work, we have investigated the excited-state intermolecular proton transfer (ESInterPT) reaction occurring through methanol-assisted molecules on the cyclic hydrogen bonds of the $7AI(MeOH)_n$ (when n=1-3) complexes. Detailed information of the ground-state structures has been acquired prior to dynamics simulation. Thus, on-the-fly dynamics simulation [59-60,62,68-69] is been employed to obtain the theoretically useful information of the $7AI(MeOH)_{n=1-3}$ clusters. We have presented both static and dynamics calculations in different methanol clusters. The reaction pathways in which the ESPT occurs through the $S_{\pi\pi^*}$ state for the $7AI(MeOH)_{n=1-3}$ complexes are also revealed. The detail of quantum dynamics simulation is analyzed and discussed.

2.2 Methods

2.2.1 Ground-state optimizations

The structures of $7AI(MeOH)_{n=1-3}$ complexes ground state were optimized in the gas phase with quantum chemical TURBOMOLE 5.10 program package [70-71]. The resolution-of-the-identity approximation [46] for the electron repulsion integrals and algebraic diagrammatic construction [47] through second order method, RI-ADC(2), was used for geometry optimizations. For polyatomic molecules, the ADC(2) calculations gave almost the same accuracy as obtained by coupled-cluster singles-and-doubles (CC2) model [49] and also requires less consuming time for

calculations than that of CC2 [59]. The split valence polarized (SVP) basis set [72] was assigned to heavy atoms and to hydrogen atoms involved in the hydrogen-bonded network, whereas the split valence (SV(P)) basis set was assigned to the remaining hydrogen atoms in the complexes. This mixed basis set, which will be referred throughout this study as SVP-SV(P), is designed to keep the computational costs for the dynamics at an acceptable level, but still providing accurate results for the 7AI and methanol systems. The minimum character of all optimized structures of $7AI(MeOH)_{n=1-3}$ were confirmed by normal mode analysis at the same basis set level, also further used for excited-state dynamics simulations.

2.2.2 Excited-state dynamics simulations

Classical dynamics simulations were carried out for the $7AI(MeOH)_{n=1-3}$ complexes on the first-excited state (S_1) energy surface. The ground-state geometries of each complex were prepared prior to initial condition generation. The initial conditions were generated using a harmonic-oscillator Wigner distribution for each normal mode, as implemented in the NEWTON-X program package [68,73] interfaced with the TURBOMOLE program. A hundred trajectories for each complex were simulated with a time step of 1 fs and the maximum time up to 300 fs for adiabatic excitation of investigating the ESInterPT/HT reactions. All trajectories of the ESPT/HT reactions were viewed using MOLDEN program [74] to analyze the different types of reactions. For a selected trajectory of each complex, we compared the energies ($kcal.mol^{-1}$) of the ground and excited states for characteristic stationary points along the reaction pathways namely normal (N), intermediary structure (IS), and tautomer (T). We employed molecular orbitals characterization of the different

electronic transitions to verify the PT or HT pathways involving in the reactions. Furthermore, a statistical analysis in the NEWTON-X program was also carried out to give detailed properties (e.g. energies and internal coordinates) which were used to obtain time evolution of the PT/HT reactions along the hydrogen-bonded network.

2.3 Results and discussion

2.3.1 Ground-state optimizations

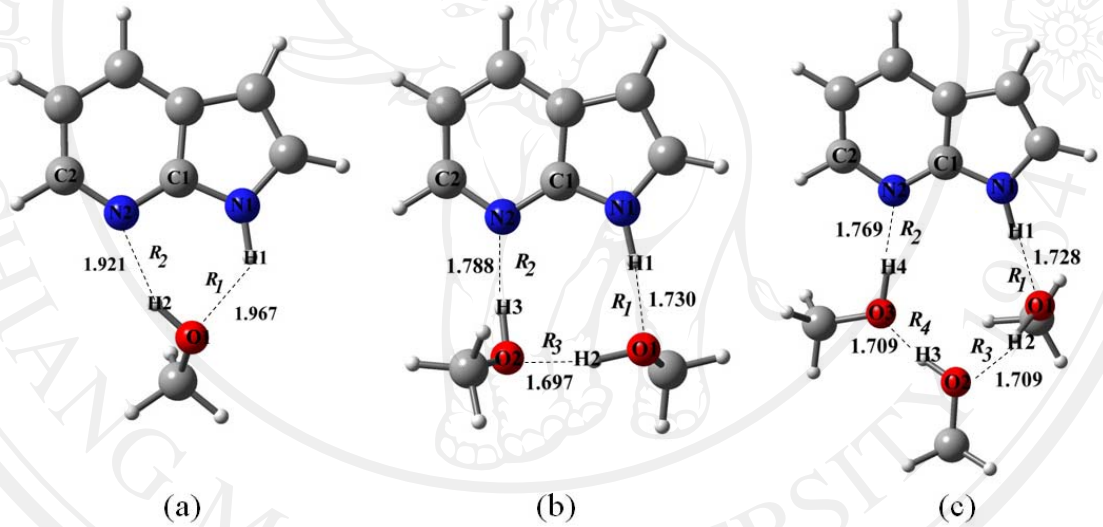

Figure 2.2 The ground-state optimized structures of 7AI(MeOH)$_n$ (when n=1-3) complexes at RI-ADC(2)/SVP-SV(P) level. Numbering atoms for intermolecular hydrogen bonds to methanol molecules (a) 7AI(MeOH)$_1$ (b) 7AI(MeOH)$_2$ and (c) 7AI(MeOH)$_3$. Intermolecular hydrogen-bonded interactions are shown in dashed lines (Å)

The optimized structures of 7AI with methanol clusters are depicted in Figure 2.2 with numbering atoms of intermolecular hydrogen-bonded networks. In order to

understand the surrounding cooperative methanol molecules on the intermolecular hydrogen bonds of the complexes, the ground-state structures of $7AI(MeOH)_{n=1-3}$ complexes were optimized using RI-ADC(2)/SVP-SV(P) level. Intermolecular hydrogen bonds between 7AI and methanol molecules presented in dashed lines, selected distances, and dihedral angles are summarized in Table 2.1.

Table 2.1 Summary of intermolecular hydrogen bonds and selected distances (Å) and øN1C1N2C2 dihedral angles (°) of the ground-state structures performed at RI-ADC(2)/SVP-SV(P) level (MP2 level in parenthesis [31])

	Complex		
	$7AI(MeOH)_1$	**$7AI(MeOH)_2$**	**$7AI(MeOH)_3$**
R_1	1.967	1.730	1.728
	(2.02)	(1.81)	(1.78)
R_2	1.921	1.788	1.769
	(1.94)	(1.80)	(1.76)
R_3	-	1.697	1.709
		(1.74)	(1.72)
R_4	-	-	1.709
			(1.70)
N1–O1	2.799	2.765	2.768
O^a–N2	2.820	2.767	2.768
O1–O2	-	2.661	2.675
O2–O3	-	-	2.674
ø	179.9	179.8	180.0

[a]O1 for one methanol in Figure 2.2a,
O2 for two methanol in Figure 2.2b,
and O3 for three methanol in Figure 2.2c.

One methanol molecule is added into 7AI molecule forming a 7AI(MeOH)$_1$ complex as shown in Figure 2.2a. It is found that the 7AI acts properly as a proton donor (pyrrole ring) and a proton acceptor (pyridine ring). Typically, there are two intermolecular hydrogen bonds labeled as R_1(H1···O1) with bond distance of 1.967 Å and R_2(H2···N2) with bond distance of 1.921 Å. The SVP basis set assigned to atoms involving in the hydrogen-bonded network is able to describe the nature of hydrogen bond well, resulting in intermolecular hydrogen bond formation between 7AI and methanol.

When two methanol molecules are added into 7AI, the new complex is formed (illustrated in Figure 2.2b). The optimized structure of a 7AI(MeOH)$_2$ complex shows that there are three intermolecular hydrogen bonds in the cyclic network: first, the hydrogen bond formation between a proton donor on pyrrole ring of 7AI and the first methanol (1.730 Å), second, the second methanol to a proton acceptor on pyridine ring of 7AI (1.788 Å), and third, between two methanol molecules (1.697Å) for R_1(H1···O1), R_2(H3···N2), and R_3(H2···O2), respectively. By increasing the number of methanol molecules, the intermolecular hydrogen bonds become stronger (the hydrogen bonds are shorter) due to dispersion interaction between 7AI and methanol. Both R_1 and R_2 of 7AI(MeOH)$_2$ cluster are shorter than those of 7AI(MeOH)$_1$ complex by 0.237 and 0.133 Å, respectively, indicating that the number of methanol molecules plays a role in structural stability.

Moreover, the optimized structure of a 7AI(MeOH)$_3$ cluster as shown in Figure 2.2c has four intermolecular hydrogen bonds (the dashed lines) as R_1(H1···O1), R_2(H4···N2), R_3(H2···O2), and R_4(H3···O3), with bond distances of 1.728, 1.769, 1.709, and 1.709 Å, respectively. For the hydrogen bonds between two methanol (R_3

and R_4), bond distances are the same. However, R_3 bond is longer than that of the 7AI(MeOH)$_2$ cluster by only 0.01 Å. Therefore, increasing number of methanol molecules certainly increases the intermolecular hydrogen bond strength between 7AI and methanol.

The study from IR-dip spectra [31] showed that the cooperative effect of hydrogen bond formation in the further sites may be saturated in 7AI(MeOH)$_3$. In addition, the optimizations of three clusters at RI-ADC(2)/SVP-SV(P) level showed that the intermolecular hydrogen bonds are slightly shorter than previously reported by Sakota *et al*. computed at MP2 level (Table 2.1). For example, R_1 and R_2 bonds of a 7AI(MeOH)$_1$ cluster show shorter intermolecular hydrogen bonds by 0.05 and 0.02 Å, respectively, as well as 7AI(MeOH)$_2$ complex with R_1(0.08 Å), R_2(0.01 Å), and R_3(0.04 Å) bonds. Hydrogen bonds R_1 and R_3 of 7AI(MeOH)$_3$ show shorter distances by 0.05 and 0.01 Å, whereas R_2 and R_4 bonds show slightly longer distances only 0.01 Å. The 7AI structure for each cluster is totally planar confirmed by dihedral angle (øN1C1N2C2) at 180° and no twist of its structure. When the dynamics simulations are performed, the 7AI structure should not be twisted because of its structural rigidity.

Structural stability of the 7AI and methanol clusters in different conformations could affect the energy barrier in the ground state, so distances between heavy atoms are considered and found that N1O1, O^{a}N2, O1O2, and O2O3 are around 2.67-2.82 Å (Table 2.1), i.e. they are quite afar. Since the N1O1 distance of the 7AI(MeOH)$_2$ cluster is the shortest distance (2.765 Å), this suggests that the barrier height in the ground state be lowest about 47.20 kcal.mol^{-1} along this reaction coordinates. However, the N1O1 distance of the 7AI(MeOH)$_1$ and 7AI(MeOH)$_3$ clusters is slightly

longer than that of the $7AI(MeOH)_2$ so the barrier reactions of these complexes are certainly higher. These optimized structures of the $7AI(MeOH)_{n=1-3}$ complexes at RI-ADC(2)/SVP-SV(P) level will be used for excited-state dynamics simulations showing the excited-state double, triple, and quadruple PT/HT reaction when n=1, 2, and 3, respectively, to obtain detailed information about the PT/HT dynamics properties.

2.3.2 Excited-state dynamics simulations

One hundred trajectories of on-the-fly dynamics simulations are initiated for each complex to investigate the PT/HT pathway. The analysis using simulation times up to 300 fs should reveal the mechanism including pre- and post-PT/HT processes. By definition, the PT/HT time from atom X to atom Y is taken as the time for which the distance X–H becomes equal the distance H–Y [60,62,67].

Table 2.2 Summary of excited-state dynamics analysis of $7AI(MeOH)_{n=1-3}$ complexes

Complex	Reaction[b]		Probability[c]	Time (fs)			
	ESPT	No		PT1	PT2	PT3	PT4
$7AI(MeOH)_1$	54	46	54	71	84	-	-
				(1.361)	(1.379)		
$7AI(MeOH)_2$	67	33	67	57	70	83	-
				(1.297)	(1.295)	(1.341)	
$7AI(MeOH)_3$	26	74	26	66	77	83	84
				(1.301)	(1.229)	(1.270)	(1.338)

[b]Unit in trajectory, [c]The reaction probability (%),
Average distance (Å) of X–H and H–Y intersection for each PT (in parenthesis).

The trajectories for each complex were classified and divided into three types of reactions: ESPT reaction, no reaction, and failed trajectories, as summarized in Table 2.2.

For selected trajectories, we have compared the energies (kcal.mol^{-1}) of the ground (S_0) and excited states ($S_{\pi\pi^*}$ and $S_{\pi\sigma^*}$) for characteristic stationary points along the reaction pathways (Table 2.3) namely normal (N), intermediary structure (IS), and tautomer (T) or each complex.

Table 2.3 Relative ground (S_0) and excited states ($S_{\pi\pi^*}$, $S_{\pi\sigma^*}$) energies (kcal.mol^{-1}) of selected trajectories of each complex for characteristic stationary points of normal (N), intermediary structure (IS), and tautomer (T) along the reaction pathways

State	Form	Complex		
		7AI(MeOH)$_1$	**7AI(MeOH)$_2$**	**7AI(MeOH)$_3$**
S_0	N	0.00	0.00	0.00
	IS	57.02	47.20	49.58
	T	15.81	10.85	13.83
$S_{\pi\pi^*}$	N	94.09	119.32	99.86
	IS	139.03	123.57	142.08
	T	94.96	98.30	88.99
$S_{\pi\sigma^*}$	N	194.23	189.54	149.99
	IS	237.66	227.29	193.00
	T	201.90	206.30	184.63

Performed at RI-ADC(2)/SVP-SV(P) level

The potential energy diagram of a selected trajectory for 7AI(MeOH)$_1$ cluster (Figure 2.3) shows that $S_{\pi\sigma^*}$ lies above $S_{\pi\pi^*}$ state over 100 kcal.mol^{-1} confirmed by no crossing between $S_{\pi\pi^*}$ and $S_{\pi\sigma^*}$ states and all trajectories of our investigation take place only $S_{\pi\pi^*}$ called PT process.

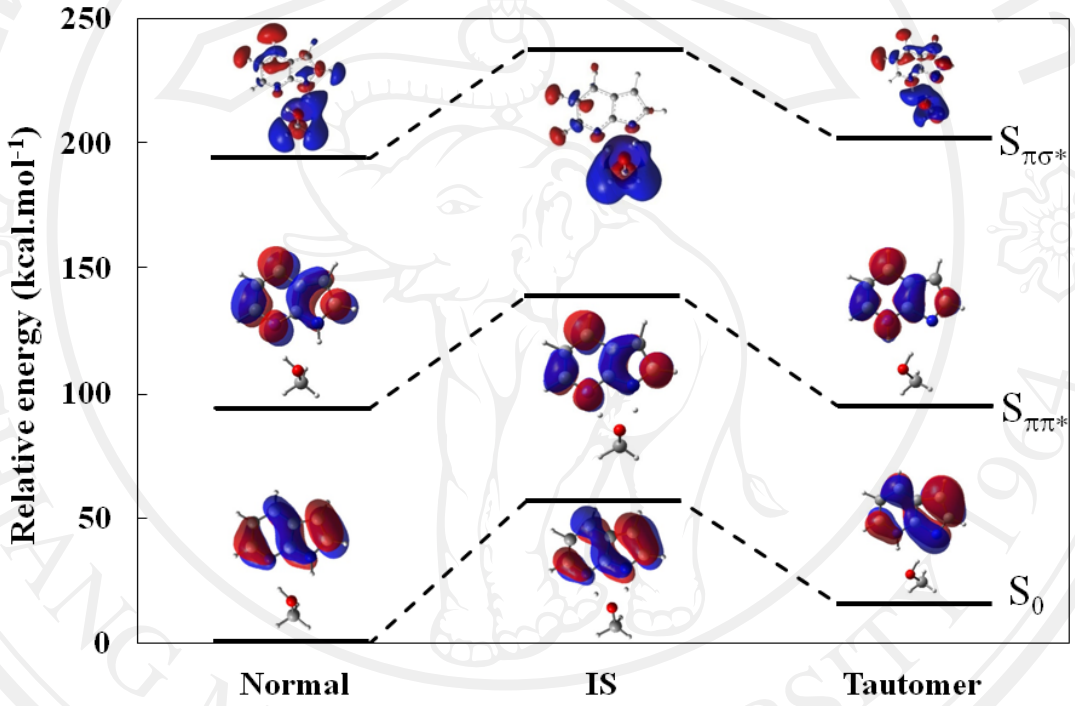

Figure 2.3 Potential energy diagram of a selected trajectory for 7AI(MeOH)$_1$ complex at ground state (S_0) and excited states ($S_{\pi\pi^*}$, $S_{\pi\sigma^*}$) performed at RI-ADC(2)/SVP-SV(P) level

The potential energy diagram of a selected trajectory for 7AI(MeOH)$_2$ cluster (Figure 2.4) shows that $S_{\pi\sigma^*}$ lies above $S_{\pi\pi^*}$ state over 100 kcal.mol^{-1} confirmed by no crossing between $S_{\pi\pi^*}$ and $S_{\pi\sigma^*}$ states and all trajectories of our investigation take place only $S_{\pi\pi^*}$ called PT process. In particular, two methanol molecules are able to

induce the ESPT reaction well with less energy crossing in the excited state. The barrier height of the selected trajectory for the 7AI(MeOH)$_2$ complex is very low (4.25 kcal.mol^{-1}), whereas other complexes have higher barrier by ten times compared with 7AI(MeOH)$_2$ complex.

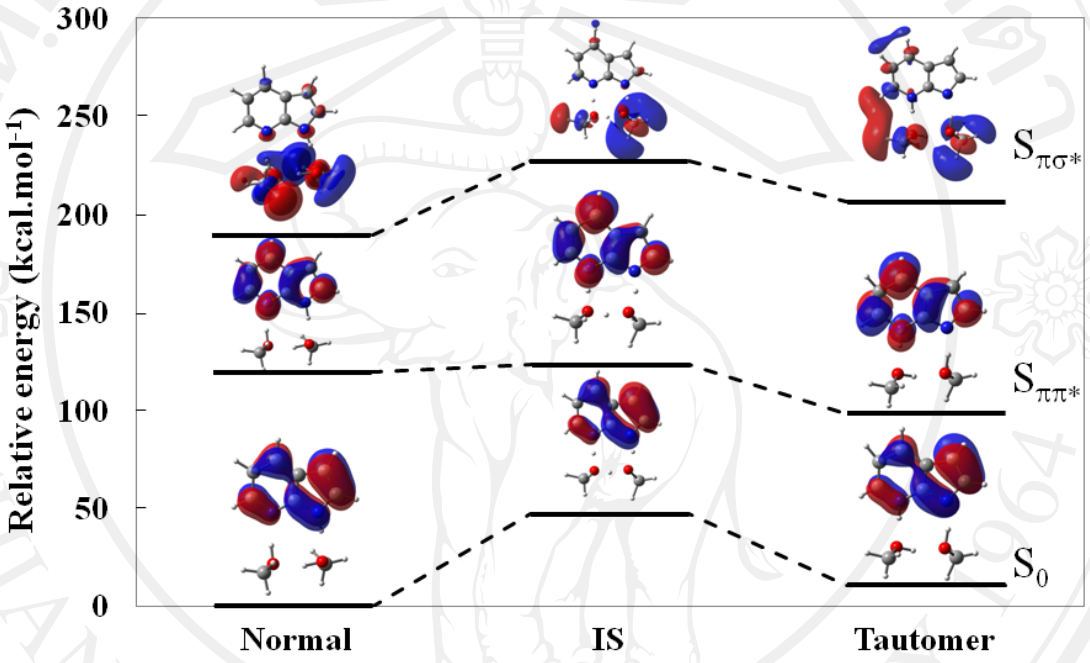

Figure 2.4 Potential energy diagram of a selected trajectory for 7AI(MeOH)$_2$ complex at ground state (S_0) and excited states ($S_{\pi\pi^*}$, $S_{\pi\sigma^*}$) performed at RI-ADC(2)/SVP-SV(P) level

The potential energy diagram of a selected trajectory for 7AI(MeOH)$_3$ cluster (Figure 2.5) shows no crossing between $S_{\pi\pi^*}$ and $S_{\pi\sigma^*}$ states. All trajectories of our investigation take place only $S_{\pi\pi^*}$ called PT process. For three methanol molecules, they can promote the ESPT reaction well but less efficient than that of two methanol. However, the processes in 7AI(MeOH)$_{n=1-3}$ complexes are most likely the ESPT pathway.

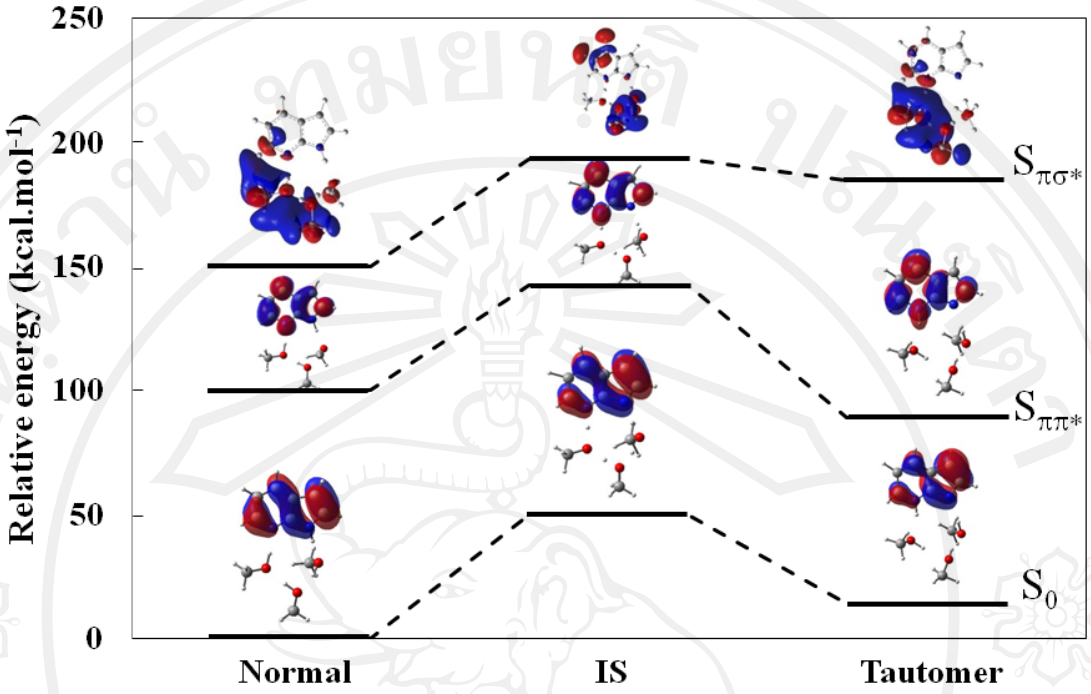

Figure 2.5 Potential energy diagram of a selected trajectory for 7AI(MeOH)$_3$ complex at ground state (S_0) and excited states ($S_{\pi\pi^*}$, $S_{\pi\sigma^*}$) performed at RI-ADC(2)/SVP-SV(P) level

In order to determine which kind of reaction, either ESPT or ESHT takes place after the photoexcitation, the relative energies of the ground and excited states of the target systems are computed. These states play a key role in determining the nature of the excited-state reactions since the ESPT occurs on the $S_{\pi\pi^*}$ state, whereas the ESHT occurs on the $S_{\pi\sigma^*}$ states. If these $S_{\pi\pi^*}$ and $S_{\pi\sigma^*}$ states are crossing, the trajectories may stop due to an error in vertical excitation section for the dynamics [60]. Thus, this investigation focuses on only the $S_{\pi\pi^*}$ state that gives detailed picture of the ESPT mechanism.

2.3.2.1 7AI(MeOH)$_1$ complex

From 100 trajectories of 7AI(MeOH)$_1$ cluster, only 13 trajectories have stopped. From total 87 trajectories, 54 of them showed excited-state double proton transfer (ESDPT) reaction but the PT process did not take place during the simulation time in 33 trajectories. However, back-PT reaction was also observed in some trajectories. Thus, the reaction probability is 54%.

The details of the PT process can be illustrated by means of a selected trajectory (Figure 2.6). The numbering atom is the same as defined in Figure 2.2a. A normal (N) form is observed at 0 fs. The H1 atom departs from pyrrole ring of 7AI to O1 atom of methanol (PT1) at 42 fs, then H2 atom of methanol moves to N2 acceptor of 7AI molecule (PT2) at 60 fs until the tautomer (T) form is achieved within 78 fs.

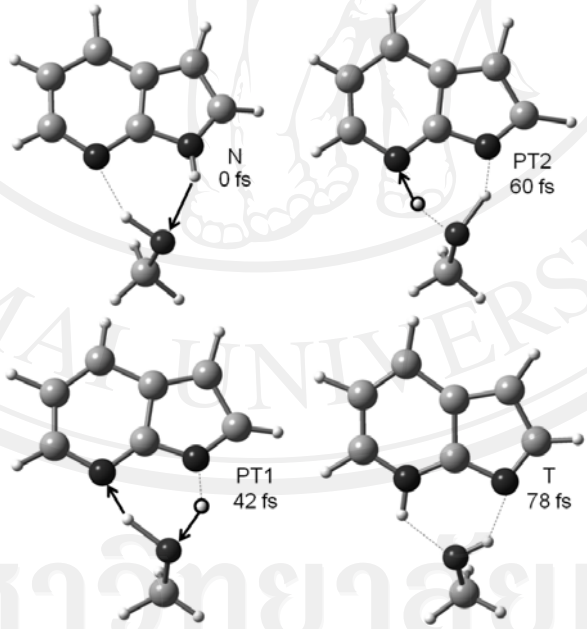

Figure 2.6 An on-the-fly dynamics simulation of a selected trajectory of a 7AI(MeOH)$_1$ complex showing time evolution of the ESDPT reaction through hydrogen-bonded network within 78 fs. Normal (N), Proton transfer (PT), and Tautomer (T)

Average values for energy and geometric parameters for the 54 trajectories following the ESDPT reaction as shown in Figure 2.7. The evolution of the average

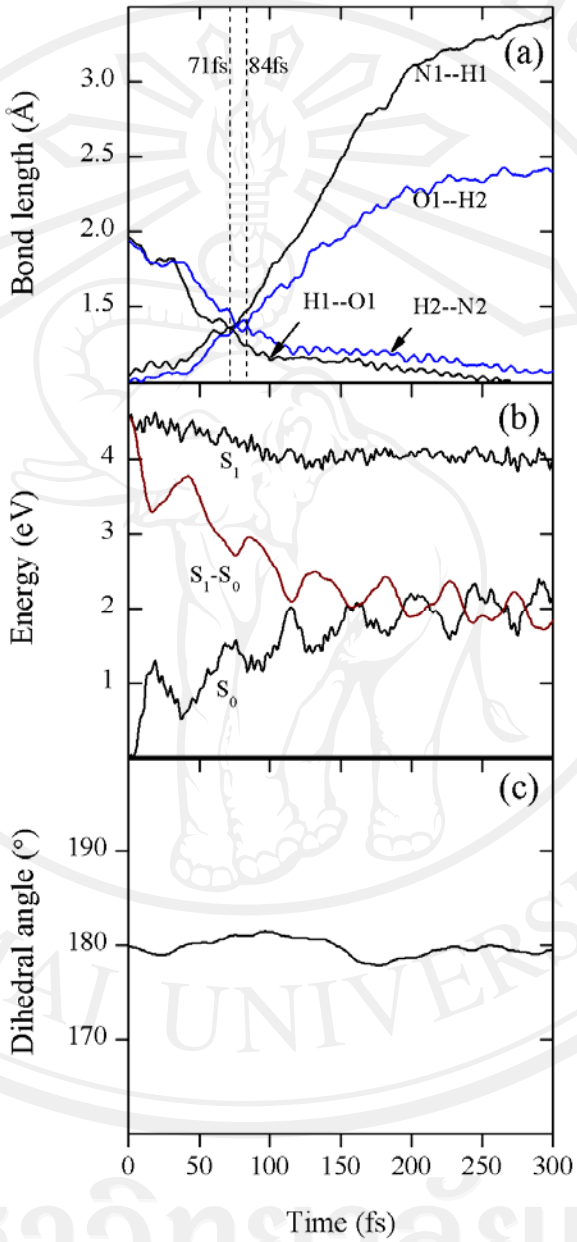

Figure 2.7 Average values over 54 trajectories of 7AI(MeOH)$_1$ complex (a) Average breaking and forming bonds showing time evolution (b) Average relative energies of excited state (S_1), ground state (S_0), and energy difference of S_1 and S_0 state (S_1-S_0) (c) Average dihedral angle of N1C1N2C2

values of two breaking bonds (N1–H1 and O1–H2) and two forming bonds (H1···O1 and H2···N2, is shown in Figure 2.7a. The intersection between the curves indicates that the first PT occurs at 71 fs when N1–H and H1–O1 bond lengths are equal to 1.361 Å, while the second PT occurs at 84 fs when O1–H2 and H2–N2 are equal to 1.379. (These values are collected in Table 2.2) Figure 2.7b shows that the average energy difference between S_1 and S_0 gradually decreases in the first 100 fs. After that, the average energy difference is still higher than 2 eV suggesting that the structure of 7AI be planar throughout the process [60]. This planarity of 7AI skeleton is confirmed by average value of the dihedral angle N1C1N2C2, which remains around 180º throughout the simulations as shown in Figure 2.7c.

2.3.2.2 7AI(MeOH)$_2$ complex

The excited-state triple proton transfer (ESTPT) reaction occurred in 67 out of 100 trajectories, while no reaction was observed in 27 trajectories and 6 trajectories failed. Therefore, the probability is 67% which is higher than that of 7AI(MeOH)$_1$ complex (see Table 2.2). A selected trajectory (Figure 2.8) reveals that the ESTPT reaction takes place within 75 fs.

The important numbering atoms assigned in Figure 2.2b are also adapted to describe this ESTPT reaction. Starting from normal form (N) at 0 fs, the process is summarized in the following three steps: (1) H1 departs from N1 to O1 (PT1) at 42 fs, (2) H2 moves from O1 to O2 of methanol (PT2) at 52 fs, and (3) H3 leaves from O2 of methanol to N2 of 7AI molecule (PT3) at 57 fs until the tautomerization (T) with methanol assistance is reached. The complete ESTPT reaction is obtained after 57 fs.

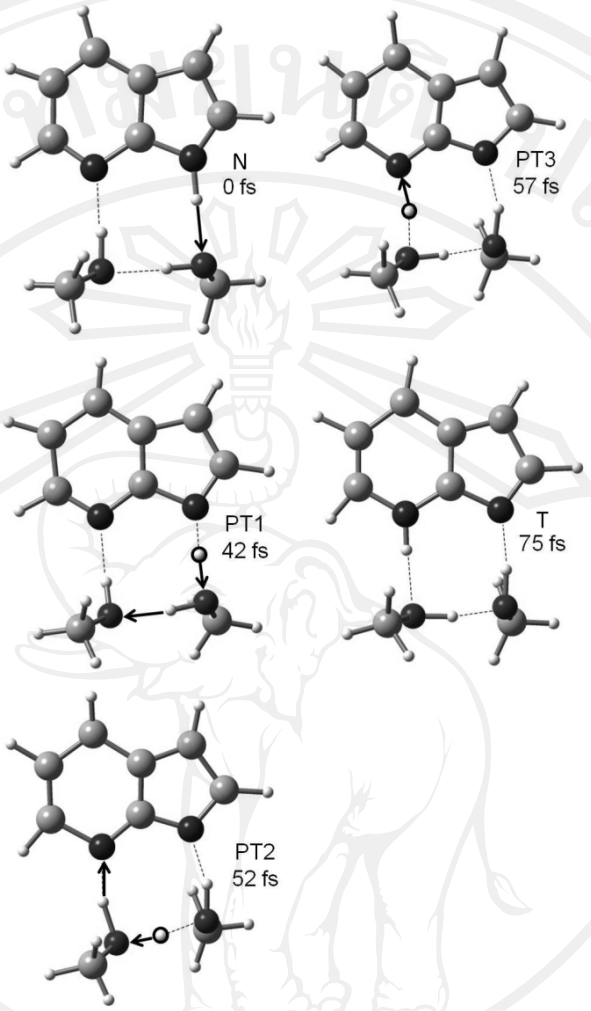

Figure 2.8 An on-the-fly dynamics simulation of a selected trajectory for a 7AI(MeOH)$_2$ complex showing time evolution of the ESTPT reaction through hydrogen-bonded network within 75 fs. Normal (N), Proton transfer (PT), and Tautomer (T)

Simultaneously, the average values of the complementary forming bonds decrease. The first PT process occurs at 57 fs when the average N1–H and H1–O1 distances are equal to 1.297 Å. The distance between the N1 and O1 atoms of 7AI(MeOH)$_2$ cluster when the proton is transferred is shorter than that of the 7AI(MeOH)$_1$ by 0.064 Å. The

proton of 7AI(MeOH)$_2$ cluster can easily move to proton acceptor because of the lower barrier.

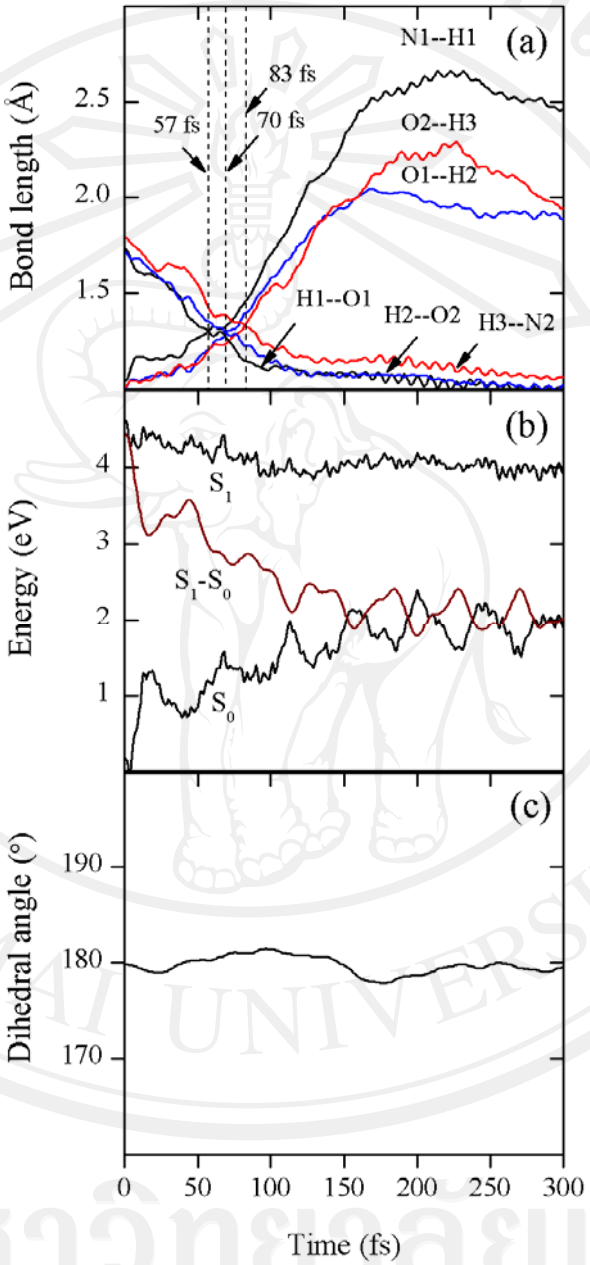

Figure 2.9 Average values over 67 trajectories of 7AI(MeOH)$_2$ complex (a) Average breaking and forming bonds showing time evolution (b) Average relative energies of excited state (S_1), ground state (S_0), and energy difference of S_1 and S_0 state (S_1-S_0) (c) Average dihedral angle of N1C1N2C2

The second proton transfers to another methanol at 70 fs when the average O1–H2 and H2–O2 distances are equal to 1.295 Å. The last PT occurs at 83 fs when the average O2–H3 and H3–N2 distances are equal to 1.341 Å (collected in Table 2.2). From 67 trajectories, the different time evolution increases 13 fs for each PT indicating that stepwise mechanism is preferable. Initially, the relative energy difference of S_1-S_0 gradually decreases. After complete PT process, average relative energy difference is still higher than 2 eV (Figure 2.9b) suggesting that the structure be planar throughout the PT process. In addition, average dihedral angle (N1C1N2C2) of 7AI is also 180º (Figure 2.9c) confirming that its skeleton structure is almost planar.

2.3.2.3 7AI(MeOH)$_3$ complex

For 7AI(MeOH)$_3$, there are four hydrogen bonds in the cyclic network. We found that 26 trajectories exhibit the excited-state quadruple proton transfer (ESQPT) reaction, while 60 trajectories exhibit no reaction. Fourteen trajectories failed. Thus, the PT reaction probability of this complex is 30% (in Table 2.2). The important numbering atoms assigned in Figure 2.2c are also adapted to describe this ESQPT reaction. A selected trajectory of 7AI(MeOH)$_3$ cluster (Figure 2.10) exhibits the ESQPT reaction as the proton moves along the hydrogen-bonded network. The normal form (N) exists at 0 fs, the first (PT1), second (PT2), third (PT3), and fourth (PT4) PT processes occur at 65, 89, 92, and 95 fs, respectively, until the tautomer (T) is formed. As the same criteria used in 7AI(MeOH)$_{n=1,2}$ complexes, we found that for 7AI(MeOH)$_3$ the crossing lines between average breaking and forming bonds (Figure 2.11a) are at 66 (N1–H1 = H1–O1), 77 (O1–H2 = H2–O2), 83 (O2–H3 = H3–O3) and

84 fs (O3–H4 = H4–N2) with bond distances of 1.301, 1.299, 1.270, and 1.338 Å, respectively, indicating PT in each step is taking place. All time differences of 7AI(MeOH)$_3$ are less than 10 fs implying that concerted mechanism is more favorable for this cluster. Average relative energy difference is above 2 eV (Figure 2.11b) and

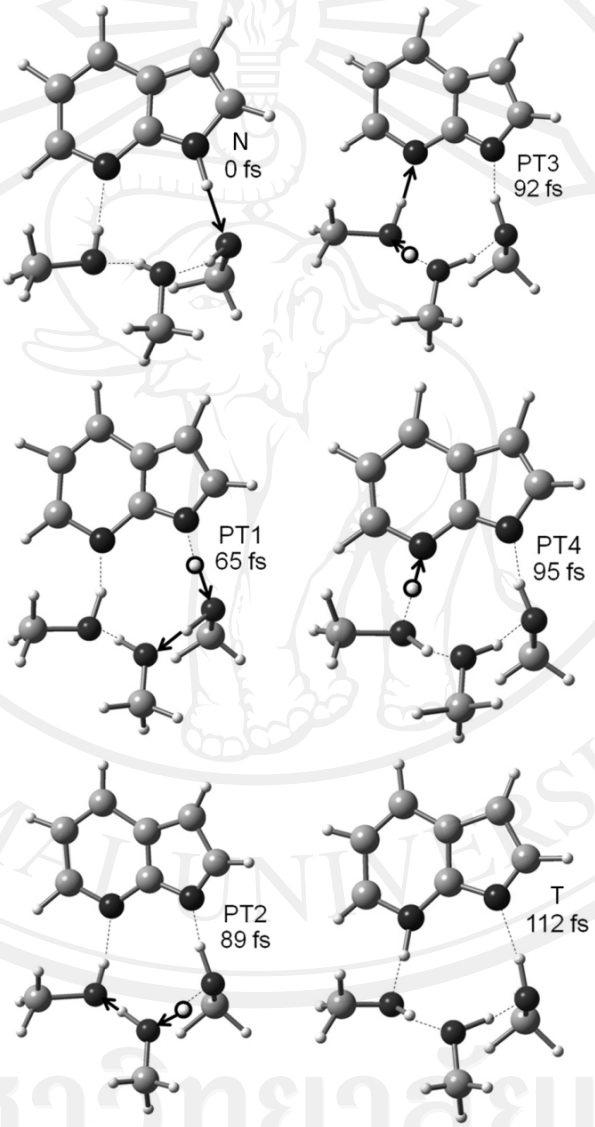

Figure 2.10 An on-the-fly dynamics simulation of a selected trajectory for a 7AI(MeOH)$_3$ complex showing time evolution of the ESQPT reaction through hydrogen-bonded network within 112 fs. Normal (N), Proton transfer (PT), and Tautomer (T)

dihedral angle is 180° indicating that planarity of 7AI is maintained with no twist in its structure throughout the simulation time (Figure 2.11c).

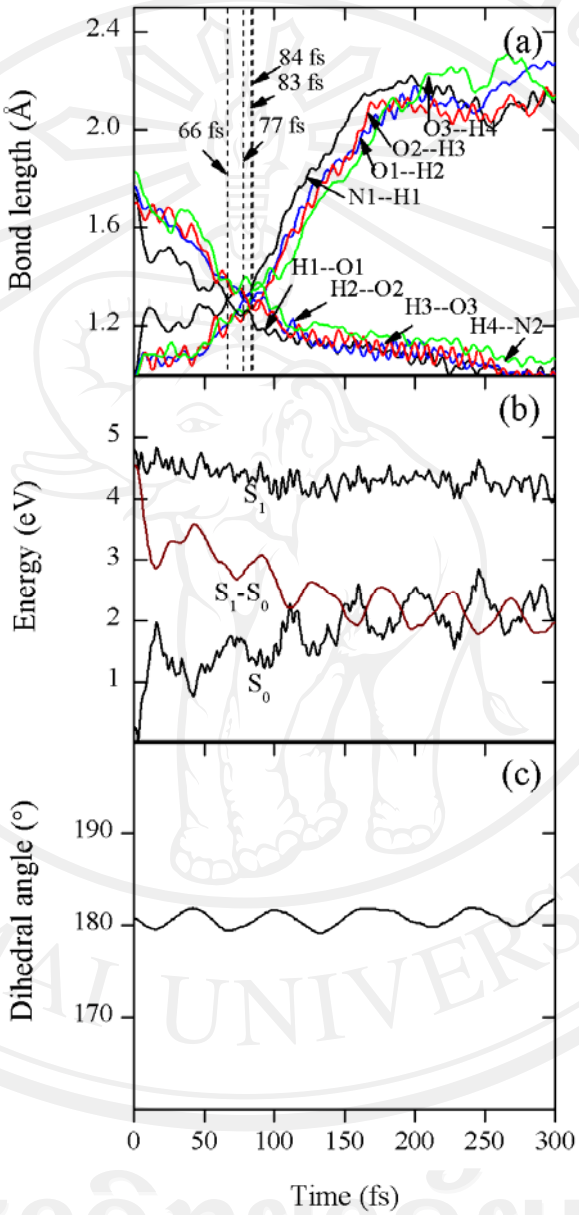

Figure 2.11 Average values over 26 trajectories of 7AI(MeOH)$_2$ complex (a) Average breaking and forming bonds showing time evolution (b) Average relative energies of excited state (S_1), ground state (S_0), and energy difference of S_1 and S_0 state (S_1-S_0) (c) Average dihedral angle of N1C1N2C2

The methanol-assisted molecules play an important role in structural stability of the 7AI(MeOH)$_{n=1-3}$ complexes. Increasing the number of methanol molecules, the intermolecular hydrogen bonds between 7AI and methanol molecules become stronger due to the attractive force interaction between them. This effect can possibly shift reaction barrier and probability of the PT reaction.

2.3.3 Reaction barriers and proton transfer types

The relative energies of the ground (S_0) and excited states ($S_{\pi\pi^*}$, $S_{\pi\sigma^*}$) of selected trajectories for all clusters are listed in Table 2.3. In the ground state, relative energies of normal forms are lower than those of tautomers referring that normal forms are more stable than the tautomers and the PT processes are not likely to proceed easily because of high barrier around 57.02, 47.20, and 49.58 kcal.mol^{-1} for 7AI(MeOH)$_n$ when n=1, 2, and 3, respectively. In contrast, the relative energies of normal forms after photoexcitation are higher than those of the tautomers and they can proceed to the tautomers more easily because of lower barrier height. These excited-state barrier heights are found to be 44.94, 4.25, and 42.22 kcal.mol^{-1} for 7AI(MeOH)$_n$ when n=1, 2, and 3, respectively. Thus, the barrier height of 7AI(MeOH)$_2$ cluster is the lowest energy one among the other clusters. This lowest barrier with the highest probability around 67% is due to its shortest distance between N1 and O1atoms (Figure 2.2) at 1.297 Å (Table 2.3) in which the PT is more readily translocated from the proton donor to the acceptor. However, the addition of three methanol molecules to 7AI affects the arrangement of hydrogen-bonded network. This effect could possibly deactivate PT by rising reaction barrier height so that the PT becomes less likely resulting in low probability, only 26%.

The average bond breaking and forming intersection can be used to represent PT time evolution well in dynamics simulations along the reaction pathways, either concerted or stepwise mechanisms. If time difference of each PT is less than fluctuation period time of 10 fs corresponding to normal vibration of N···H and O···H hydrogen bond stretching modes, the concerted mechanism (the proton moves continuously and very rapidly) is involved. However, time interval of each PT for the $7AI(MeOH)_{1,2}$ complexes is 13 fs implying that stepwise mechanisms are detected. Although the PT is either concerted or stepwise mechanisms, the photo-tautomerization of all complexes is achieved with short time of 84 fs. Therefore, different types of the ESPT mechanisms and also reaction probability are cluster-size selective.

2.4 Summary

We have carried out the ground-state structures of $7AI(MeOH)_n$ (when n=1-3) clusters at RI-ADC(2)/SVP-SV(P) level. We found that intermolecular hydrogen bonds between 7AI and methanol molecules increase or become stronger when the number of methanol increases. The excited-state investigations of these complexes have revealed that the ESPT reactions are ultrafast reactions. The ESPT takes place along the PT pathways confirmed by no crossing between $S_{\pi\pi^*}$ and $S_{\pi\sigma^*}$ states within 84 fs. The time intervals of each PT become shorter and more favorable concerted mechanism due to shorter distances between heavy atoms in the cyclic network. In this case, the proton can migrate easily from the proton donor to the acceptor so that the energy barrier height in the excited state is low. The ESInterPT process is a cluster-size selective even though the PT cycle of all complexes is finished within

84 fs. Especially, two methanol molecules can assist and promote the ESTPT reaction with the most efficient one among the other complexes. In addition, this study has revealed that methanol assistance plays an important role in excited-state dynamics simulation insight into the PT pathway. Thus, all these complexes can be used as a good prototype for the excited-state intermolecular PT process with an effective RI-ADC(2) method at sufficient small basis set.